Advanced Energy Conversion for Sodium-Cooled Fast Reactors

J. J. Sienicki, A. Moiseytsev, Q. Lv, and C. D. Gerardi

Argonne National Laboratory, Argonne, Illinois, United States of America

E-mail contact of main author: sienicki@anl.gov

Abstract. Advanced energy conversion using the supercritical carbon dioxide (sCO_2) Brayton cycle continues to receive significant support in the U.S. from the U.S. DOE and U.S. industry. Its main benefits for SFRs are improvement of SFR economics and elimination of the need to accommodate sodium-water reactions. It has been shown that the cycle enables the economical use of dry air cooling whereby heat is rejected directly to the air atmosphere through the use of commercially available, cost effective, finned tube air coolers. Significant progress has been made in obtaining data on potential sodium-CO_2 interactions under prototypical conditions through ongoing sodium-CO_2 interaction tests indicating that sodium-CO_2 interactions are relatively benign compared to sodium-water reactions. The Plant Dynamics Code coupled to the SAS4A/SASSYS-1 SFR transient analysis code for system level steady state and dynamic analyses and optimization of sCO_2 cycles and their control strategies has been improved and is being validated through comparison with data from sCO_2 integrated cycle test loops.

Key Words: Supercritical CO_2 Brayton cycle, dry air cooling, sodium-CO_2 interactions, Plant Dynamics Code.

1. Introduction

The supercritical carbon dioxide (sCO_2) Brayton cycle continues to receive significant support in the U.S. from the United States Department of Energy (U.S. DOE) Offices of Nuclear Energy, Fossil Energy, and Energy Efficiency and Renewable Energy; the latter Office including concentrating solar power. The first applications identified for sCO_2 Brayton cycles were Nuclear Power Plants (NPPs) [1]. The main feature of a nuclear reactor is that it delivers heat over a limited temperature range at high temperature. For a Sodium-Cooled Fast Reactor (SFR), the core temperature rise of approximately 150 °C is approximately equal to the temperature drop that CO_2 undergoes inside of the power turbine as it expands from the high cycle pressure to low cycle pressure. As a result, a SFR and a recuperated sCO_2 Brayton cycle can be well matched to provide a high efficiency [1].

In the U.S., recent years have seen the generation of data from the Recompression Closed Brayton Cycle (RCBC) and Integrated System Test (IST) 0.78 MWt sCO_2 integral test loops at Sandia National Laboratories and the Naval Nuclear Laboratory, respectively. The Supercritical Transformational Electric Power (STEP) program to build and operate by 2020 a natural gas-heated 10 MWe sCO_2 Brayton cycle was recently awarded to the Gas Technology Institute and its main partners at Southwest Research Institute, where the power converter will be sited, and GE Global Research. The DOE award may be as much as $ 80,000,000 over six years augmented by cost share contributions from the industrial partners.

The sCO_2 Brayton cycle has been under development at Argonne National Laboratory (ANL) since 2002. Analyses and data continue to confirm the main benefits of the cycle for SFRs that are reduction of the SFR capital cost per unit output electrical power ($/kWe) or Levelized Cost of Electricity (LCOE) improving SFR economics (a goal of the U.S. DOE

SFR Program) and eliminating sodium-water reactions. The focus of this paper is to review selected key developments in the sCO_2 Brayton cycle for SFR applications achieved since FR13.

2. Dry Air Cooling

Initial investigations of the sCO_2 Brayton cycle assumed heat rejection to water. However, the Clean Water Act in the U.S. and its implementing regulations require limits on the effluent temperature discharged into water bodies. Heat rejection to the ambient atmosphere involving water evaporation using cooling towers or spray ponds can reduce water usage by an order of magnitude. However, water makeup is still needed for evaporative losses. Regions in the U.S. are becoming water stressed and are employing water conservation measures and alternate water sources (e.g., California, Texas, and Florida). Dry air cooling involves direct heat rejection to the ambient atmosphere. It is an answer to the risk to future power production in water stressed regions as well as the future uncertainty in the availability of water resources for power plant cooling including the effects of climate change. An added benefit of dry air cooling is siting flexibility. A power plant does not need to be sited near a body of water. Therefore, an area of development has been the use of dry air cooling with sCO_2 Brayton cycles. This has been done first for the Advanced Fast Reactor (AFR)-100 100 MWe-class SFR Small Modular Reactor (SMR) NPP [2] .

The original sCO_2 power converter conceptual design for the AFR-100 rejected heat from the CO_2 to water that rejected heat to the atmospheric heat sink through many modular commercially available cooling towers. Optimized conditions with circulating water and cooling towers obtained with the ANL Plant Dynamics Code [3] are shown in FIG. 1.

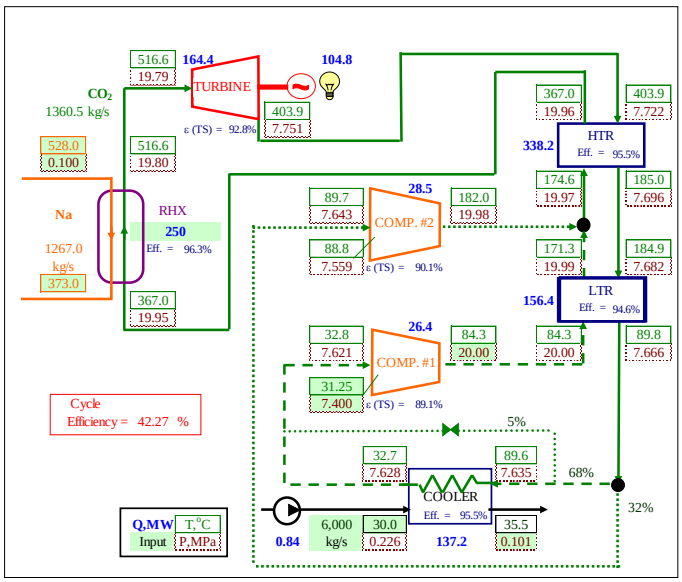

FIG 1. AFR-100 sCO_2 Brayton Cycle Optimized Conditions with Heat Rejection via Circulating Water and Cooling Towers.

The enabling technology for dry air cooling for sCO_2 power cycles are commercially available and cost effective modular finned tube air coolers such as those manufactured by Harsco Industrial [4]. Although compact diffusion-bonded heat exchangers have received

much attention for use with sCO_2 cycles, they are not cost effective as air coolers [5]. FIG. 2 illustrates a finned tube air cooler module.

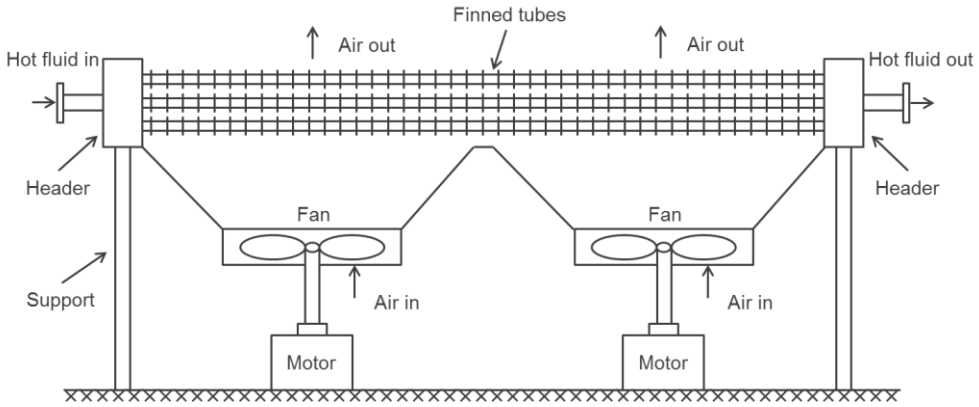

FIG. 2. Illustration of Modular Finned Tube Air Cooler.

Cooling air is forced upward by large diameter electric motor-driven fans to flow over horizontal finned tubes through which the CO_2 flows. FIG. 3 illustrates the particular Harsco design assumed in which the finned tube bundle is divided into three geometrically parallel sub-bundles each having four layers of tubes. Carbon dioxide enters the first sub-bundle from the inlet header, exits into the opposite header, enters the second sub-bundle to flow in the opposite direction, exits into another header, and enters the third sub-bundle to flow to the opposite outlet header. The specific module design incorporates three large diameter air fans. When there is more than a single modular finned tube air cooler, the CO_2 flow is assumed to be split to flow between the modules in parallel.

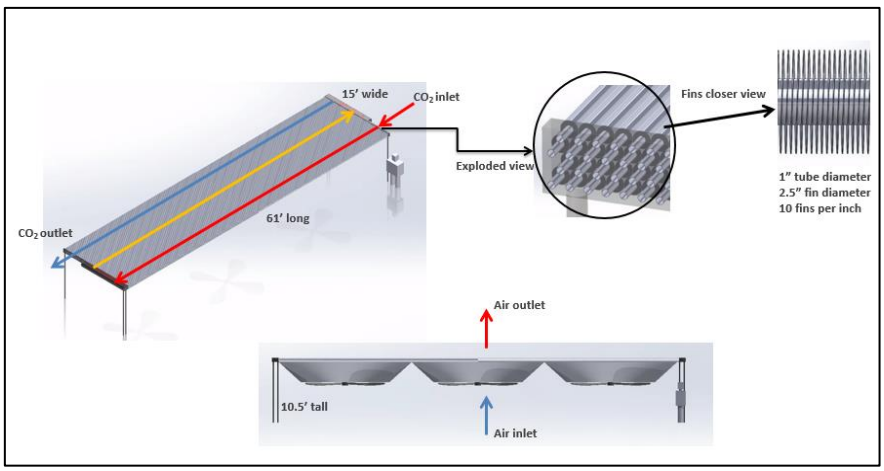

FIG. 3. Illustration of Horizontal Finned Tube Bundle and Multiple Passes for CO_2 Through Upward Air Flow.

When water cooling instead of dry air cooling is used for heat rejection from the CO_2 and assuming a circulating water heat sink temperature of 30 °C (86 °F), it is practical to cool the

CO_2 to be close to the CO_2 critical temperature and pressure (e.g., a main compressor inlet temperature and pressure of 32 °C and 7.4 MPa versus T_{crit} = 30.98 °C and P_{crit} = 7.377 MPa) through the use of compact diffusion-bonded coolers (see FIG. 1). With dry air cooling, maintaining such CO_2 conditions close to the critical temperature with 30 °C (86 °F) ambient air would require a large number (86) of Harsco modular finned tube air cooler units raising the plant capital cost.

It is necessary to re-optimize the sCO_2 Brayton cycle conditions for dry air cooling. It was decided to increase the main compressor inlet temperature to 35 °C (95 °F) and increase the pressure along the pseudocritical line to 8.2 MPa to limit the air cooler size to a practical value. This reduces the cycle efficiency. In order to offset the loss in cycle efficiency, the compressor outlet pressure is increased from 20 to 25 MPa to maintain a high efficiency. A cycle efficiency of 42.67 % is calculated with dry air cooling versus 42.27 % with water cooling. Re-optimized cycle conditions for dry air cooling are shown in FIG. 4.

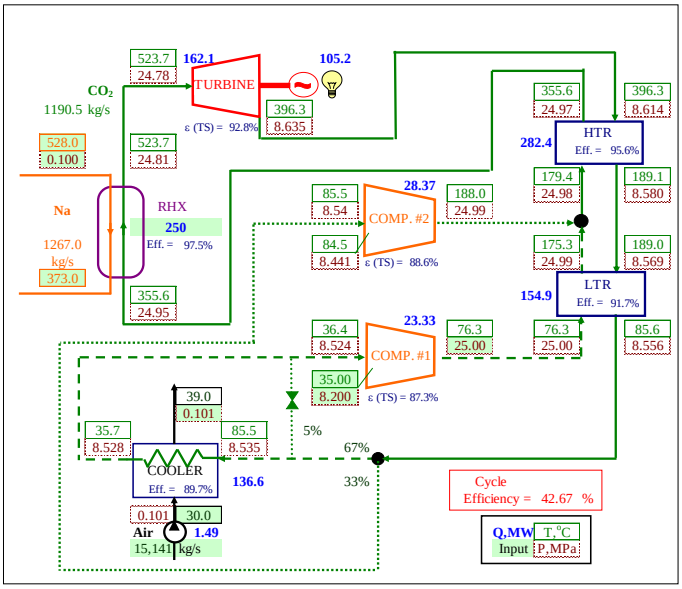

FIG. 4. AFR-100 sCO_2 Brayton Cycle Optimized Conditions with Heat Rejection via Dry Air Cooling.

The re-optimization results in different designs as well as numbers of all of the heat exchangers and turbomachinery stages in the cycle. The objective is to minimize the NPP capital cost per unit output electrical power (i.e., $/kWe). The methodology described in References [6] and [7] is applied. For the case of the modular air coolers, the design of each module is fixed as the Harsco design and only the number of modules changes. Cost quotes received from Harsco are used. As the number of cooler modules increases, the air flow area through all of the modules increases, the air flowrate in each module decreases, and the air pressure drop decreases reducing the overall electrical power requirement for the motor-driven air fans such that the plant efficiency rises. For example, FIG. 5 shows the total electrical power needed for the air fans versus the number of modules. The needed electrical power decreases as the number of modules rises. However, the total cost of all of the air cooler modules also rises. The NPP $/kWe exhibits a minimum at the optimal number of air cooler modules.

The ratio of the plant $/kWe as the number of air cooler modules is varied to the $/kWe for the optimized cycle with once-through water cooling is presented in FIG. 6. Sixty-seven Harsco modular air coolers minimize the NPP $/kWe. The estimated value for the NPP $/kWe is only 2 % greater with dry air cooling compared to once-through water cooling. This is a significant result, although the uncertainties in the cost estimation modeling are significant such that this result is also subject to significant uncertainty.

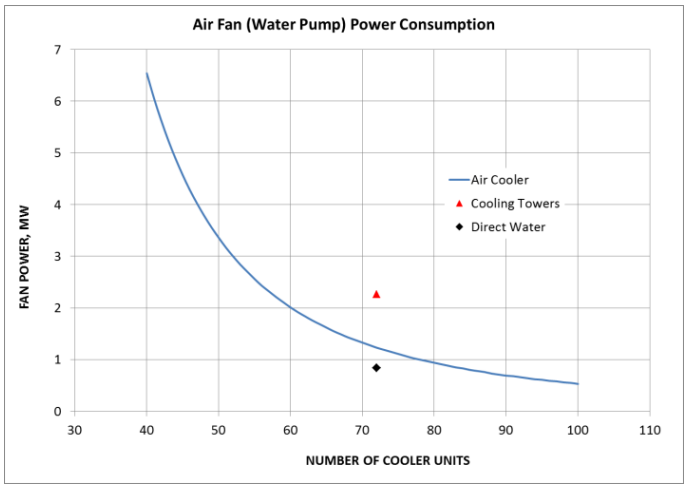

FIG. 5. Total Electrical Power Required for Air Fans versus Number of Modular Air Cooler Units.

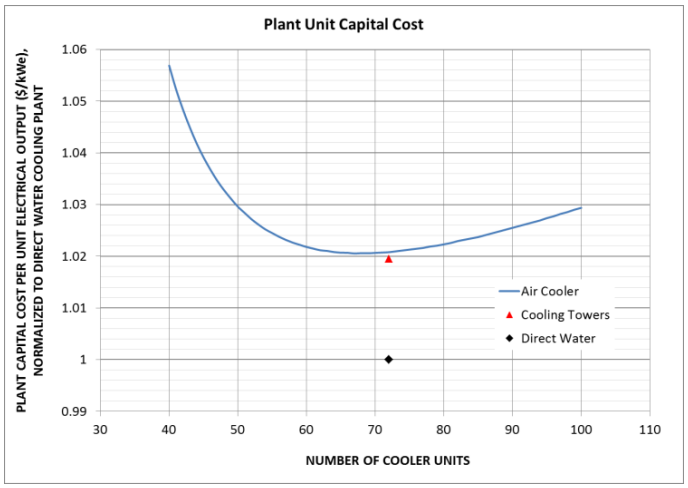

FIG. 6. Normalized NPP $/kWe versus Number of Modular Air Cooler Units.

Table I compares the re-optimized values of other cycle components and cycle conditions for dry air cooling versus water cooling. The values have been selected to independently minimize the NPP $/kWe.

TABLE I. OPTIMIZED COMPONENTS FOR DRY AIR COOLING VERSUS WATER COOLING

Component	**Design Parameter**	**Water Cooling Value**	**Dry Air Cooling Value**
Cycle	Minimum temperature	31.25 °C	35.0 °C
	Minimum pressure	7.4 MPa	8.2 MPa
	Minimum pressure	20 MPa	25 MPa
	Compressor flow split	67 %	68 %
Sodium-to-CO_2 Heat Exchanger	Configuration	Hybrid Heat Exchanger	Hybrid Heat Exchanger
	Number of units	96	84
	CO_2 side p/d	1.3	1.4
	CO_2 side plate thickness	1.6 mm	1.65 mm
High Temperature Recuperator	Configuration	Platelet PCHE	Platelet PCHE
	Number of units	48	38
	p/d, both sides	1.3	1.4
	Plate thickness, both sides	1.0	1.065
Low Temperature Recuperator	Configuration	Platelet PCHE	Platelet PCHE
	Number of units	48	48
	p/d, both sides	1.3	1.35
	Plate thickness, both sides	1.0	1.04
Turbine	Configuration	Axial flow	Axial flow
	Number of stages	6	8

3. Sodium-CO_2 Interactions

A benefit of the sCO_2 Brayton cycle is improvement of SFR economics through elimination of sodium-water reactions (SWRs) thereby eliminating equipment required to detect small water/steam leaks or mitigate against the effects of large leaks. However, sodium-CO_2 interactions can release heat and form reactions products. To use a sCO_2 Brayton cycle with a SFR, it is necessary to understand the phenomena of sodium-CO_2 interactions under prototypical SFR conditions.

It is interesting to compare the theoretical heat release rates for a SWR and a sodium-CO_2 interaction assuming release through identical postulated crack/hole areas. For a SWR, the reaction is

$Na + H_2O \rightarrow NaOH + ½H_2 – 164$ kJ/mol.

The heat release is equivalent to 9.1 MJ/kg of water/steam. The mass flux of water/steam exiting the hole is assumed to be given by the critical flowrate for saturated water steam at 15 MPa. It ranges from 26,000 to 60,000 kg/(m^2·s), as the quality on the water/steam side varies from 1.0 (all saturated steam) to 0.0 (all saturated liquid) [8]. The critical flowrate decreases as the steam becomes more superheated and increases as the water becomes more subcooled. Thus, the exothermic heat release rate flux varies from 2.4×10^{11} to 5.5×10^{11} J/(m^2·s), as the quality varies from 1.0 to 0.0.

For sodium and CO_2 at lower temperatures relevant to a sodium-to-CO_2 heat exchanger, the interaction is assumed to be [9]

$Na + CO_2 \rightarrow ¼Na_2C_2O_4 + ¼CO + ¼Na_2CO_3 – 258$ kJ/mol.

The heat release is equivalent to 5.9 MJ/kg of CO_2. The critical flowrate for sCO_2 at 20 MPa at the nominal temperatures inside of the heat exchanger can be estimated by treating the CO_2 as an ideal gas. The critical flowrate varies from 35,000 to 44,000 kg/(m^2·s), as the temperature varies from the hot to the cold end of the sodium-to-CO_2 heat exchanger. The heat release rate flux varies from 2.1×10^{11} to 2.6×10^{11} J/(m^2·s) from the hot to the cold end of the heat exchanger. Thus, the potential heat release rate estimated for a sodium-CO_2 interaction is less than but comparable with that estimated for a SWR in the saturated region of a steam generator. At lower temperatures where this equation is relevant, experiments in a stratified configuration with CO_2 above a small sodium pool revealed that there is an induction time effect whereby the onset of significant reaction is delayed (References [9] and [10]). The induction time decreases as the temperature increases [9].

At sufficiently high temperatures (above a threshold at perhaps about 500 °C), sodium and CO_2 may react according to

$^4/_3Na + CO_2 \rightarrow ⅓C + ⅔Na_2CO_3$ -349 kJ/mol.

The heat release is equivalent to 7.9 MJ/kg of CO_2. The threshold for this reaction may lie above the highest temperature attained inside of the heat exchanger. If this reaction occurs, then the estimated heat release rate flux is again comparable with that estimated for a SWR. Above the threshold temperature, reaction of sodium and CO_2 in stratified configurations has been observed to be fast and essentially instantaneous [9].

However, any similarities between SWRs and sodium-CO_2 interactions diverge after formation of the postulated same initial crack area. The sodium hydroxide formed by a SWR attacks the steel surrounding the hole enlarging the hole size due to wastage (i.e., corrosion and erosion) and increasing the water/steam release rate and the heat release rate. The hydrogen formed, due to its low atomic mass and the increased temperature, expands significantly to create significant local pressure loadings. Impingement of the SWR jet formed upon neighboring steam generator tubes or structure (e.g., the steam generator shell) together with increased temperature can cause failure propagation due to wastage resulting in additional release of water/steam from other tubes.

In contrast, there now exist independent datasets showing that the effects of sodium-CO_2 interactions upon steel structure are relatively benign. Test performed at the Korea Atomic Energy Research Institute (KAERI) investigating wastage with CO_2 have revealed that wastage effects are negligible [11]. This observation is supported by the sodium-CO_2 interactions tests performed in the SNAKE facility at ANL [12]. In none of the experiments, has attack upon or enlargement of the stainless steel injection nozzle been observed. Thus, an initial crack will not be enlarged and the heat release rate will not increase with time due to the effects of sodium-CO_2 interaction. Due to its greater atomic mass, lower mole fraction, and the low heat release rate, carbon monoxide formed causes much lower local pressure loadings than the hydrogen in a SWR.

The SNAKE data also reveals that there may be a self-plugging phenomenon whereby the formation of sodium-CO_2 reaction products self-seals the initial leak. Self-plugging has been definitively observed in two of the SNAKE experiments carried out at higher temperature. In the recent 2016_14 SNAKE experiment, sCO_2 at 20 MPa and 495 °C was injected through a 71 μm diameter stainless steel nozzle upward into an overlying 0.4 m high 10 cm diameter column of sodium at 497 °C and 0.45 MPa pressure. No CO_2 or CO was

measured leaving the top surface of the sodium column. Instrumentation included acoustic sensors that are effective in recording the noise accompanying injection of CO_2 from the nozzle. From analysis of the recorded power spectrum versus time, it is possible to deduce an estimate of the effective unobstructed nozzle diameter versus time. This is shown in FIG. 7 below. It is envisioned that the effective diameter decreases with time due to the buildup of sodium-CO_2 reaction products. The temporary increases in the effective diameter in FIG 7 might be due to local spalling of reaction products. The plugging stopped the CO_2 injection holding back the applied pressure. Self-plugging is consistent with the sodium-CO_2 reaction assumed at higher temperatures in which there are no gaseous reaction products and the reaction occurs essentially instantaneously.

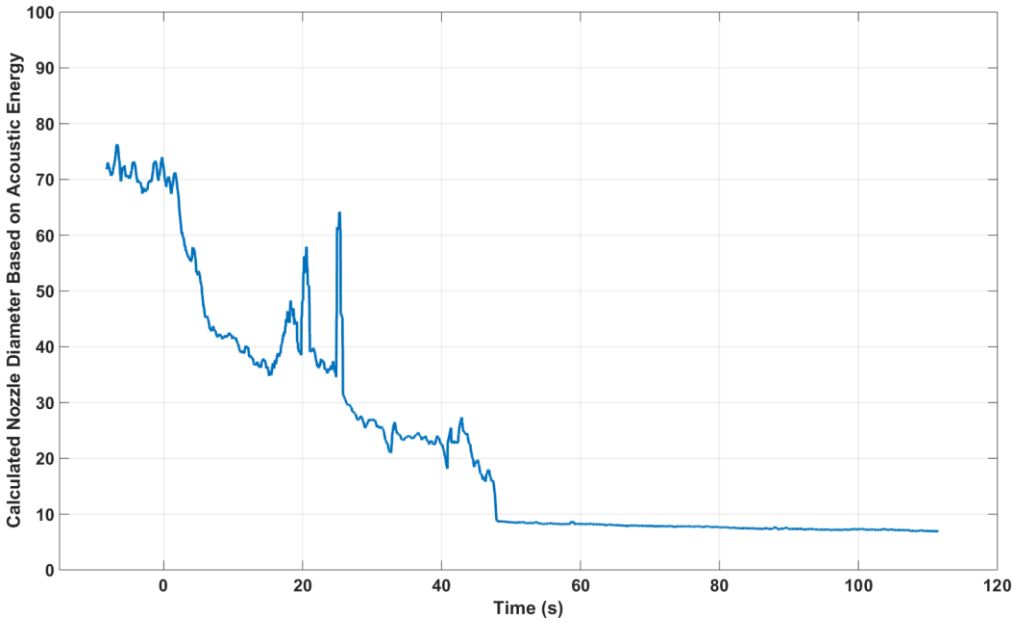

FIG. 7. Deduced Effective Injection Nozzle Diameter versus Time in SNAKE Experiment 2016_14.

FIG. 8 shows pre-test and post-test images of the injection nozzle from the earlier experiment at 500 °C in which self-plugging occurred. The reaction products were measured to be by weight 45.0 % O, 39.5 % Na, 13.1 % C, 1.9 % Fe and 0.8 % Cr.

Thus, not only do sodium-CO_2 interactions not enlarge a crack but at sufficiently high temperatures, might self-seal the opening terminating the leak. A high priority for near-term future SNAKE testing is to conduct a test at a lower temperature such as 420 °C to determine if self-plugging still occurs at temperatures significantly below 497 °C.

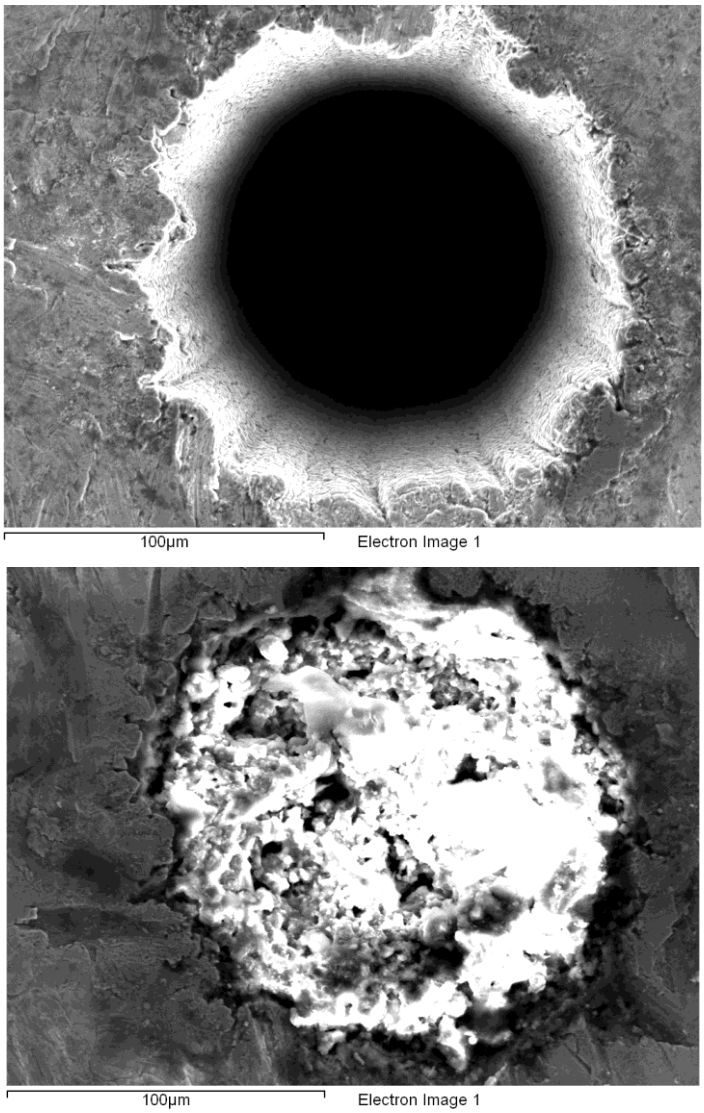

FIG. 8 Pre-Test and Post-Test Images of Nozzle Completely Plugged by Sodium-CO_2 Reaction Products.

SNAKE experiments at lower temperatures representative of the cold end of the heat exchanger as well as temperatures below those representative of the heat exchanger have thus far not shown self-plugging but the essentially complete reaction of CO_2 with sodium resulting in the formation of a porous agglomerated mass of reaction products that is less dense and floats atop the sodium column (FIG. 9). The lack of self-plugging is consistent with an induction time for the onset of significant reaction such that bubbles of CO_2/CO and surrounding sodium travel away from the nozzle before the onset of significant reaction. The tests have not shown any enlargement of the nozzles due to wastage. The results of sodium-CO_2 interaction experiments conducted at KAERI also reveal the formation of reaction products that over time blocked the sodium flow through 3 and 5 mm diameter sodium channels with significantly longer timescales for the 5 mm diameter channel ([13] and [14]). In the KAERI experiments that featured subsonic and low CO_2 injection rates, the reaction products accumulated mainly in the vicinity of the CO_2 injection nozzle [15].

The formation of solid debris that is not readily soluble in sodium may be problematic. In such a case, following the detection of CO_2 leakage into sodium, it may be desirable to isolate the CO_2 inlet and outlet lines to the heat exchanger as one of a number of steps to terminate

the reaction. The acoustic instrumentation results from the SNAKE experiments are encouraging that acoustic monitoring may be a viable approach to detection of small leakages. The lack of wastage accompanying sodium-CO_2 interactions means that the timescale in which to detect the occurrence of a CO_2 leakage may be reasonably long. Results such as those of FIG 9 are for injections of a significant cumulative mass of sCO_2 into a 10 cm diameter sodium column. The next SNAKE experiment will investigate a sCO_2 injection into a single sodium channel mocking up a 6 mm semicircular diameter sodium channel of a sodium-to-CO_2 heat exchanger.

FIG. 9. Typical Sodium-CO_2 Solid Reaction Products Inside of Sodium-CO_2 Reaction Vessel Observed in SNAKE Experiments Conducted at Lower Temperatures.

4. ANL Plant Dynamics Code

ANL's ongoing and unique historical workscope areas in the U.S. DOE Office of Nuclear Energy development of the sCO_2 Brayton cycle include the development, validation, and application of tools/computer codes for steady state and transient analysis of sCO_2 Brayton cycles, optimization of sCO_2 Brayton cycles, as well as development of control strategies for sCO_2 Brayton cycles coupled to various heat sources including nuclear power reactors. The focus of this work is the ANL Plant Dynamics Code (PDC); the word, "Dynamics," is unfortunately misleading because the code also covers steady state and off-design performance. It is currently the worldwide state-of-the-art tool for analysis of sCO_2 Brayton cycles including those coupled to SFRs. The PDC is coupled to the SAS4A/SASSYS-1 SFR transient analysis code [16] providing a capability to model the whole NPP [17].

Since FR13 [18], modeling incorporated in the PDC has been extended to include closed loop active control of the reactor (e.g., through motion of control rods and pump torques/shaft speeds in SFRs) in addition to open loop autonomous control [19], use of the sCO_2 cycle power converter for removal of reactor decay heat down to low levels of about 1 % nominal power through control of the CO_2 turbomachinery shaft speed following disconnection of the generator from the electrical grid [19], modeling for dry air cooling with finned tube air coolers and crossflow compact diffusion-bonded heat exchangers [5], and modeling needed for the specific small-scale sCO_2 test loops at Sandia National Laboratories (the

Recompression Closed Brayton Cycle, RCBC) [20] and at the Naval Nuclear Laboratory (the Integrated System Test, IST) [21]. Testing in the RCBC has been delayed due to hardware technical problems while testing at the IST is now completed.

Detailed comparison of PDC predictions versus data from the RCBC and IST have confirmed, improved, or validated the modeling for Printed Circuit Heat Exchangers (PCHEs) and shell-and-tube heat exchangers, the general turbomachinery approach in terms for turbomachinery performance maps, centrifugal compressor modeling, radial turbine modeling, although some loss models need further validation, compressibility effects exhibited by relocation of CO_2 mass from one part of the system to another during transients, as well as the general loop response and control actions during transients.

The prospect for validation using future data from the 10 MWe STEP pilot plant is exciting to contemplate as a source for data at larger scale more representative of commercial scale power converters that cannot be obtained from the small-scale facilities. In particular, data may be available for axial turbines, possibly axial compressors, and at more prototypical rotational/shaft speeds and velocity triangles. Most significantly, the data will be less subject to the drawbacks of small-scale loops by virtue of smaller windage and leakage losses better revealing other turbomachinery loss effects, smaller, in relative terms, turbomachinery leakage flows, and smaller loop heat losses by virtue of smaller surface-to-volume heat loss effects.

5. Summary

Advanced energy conversion using the supercritical carbon dioxide (sCO_2) Brayton cycle continues to receive significant support in the U.S. from the U.S. DOE and U.S. industry. Ongoing progress in the development of the sCO_2 Brayton cycle for SFR applications at ANL continues to confirm its benefits and promise. Three examples have been provided.

It has been shown through analysis that the cycle can be economically used with dry air cooling through the utilization of commercially available, cost effective, finned tube air coolers. This is especially important for future deployments in the U.S.

Although sodium-CO_2 interactions exhibit an exothermic heat release and the estimated heat release rate flux from a leak is comparable to that from a sodium-water reaction that is where similarities between the two interactions end. Recent data continues to show that sodium-CO_2 interactions are relatively benign compared to sodium-water reactions. Sodium-water reactions are accompanied by wastage of steel due to attack by the hydroxide reaction product enlarging an initial crack increasing the leakage rate, increasing the heat release rate, and causing failure propagation due to impingement upon other steam generator tubes further enhancing the leakage rate. Hydrogen reaction product creates significant local pressure loadings. In contrast, data has shown that for sodium-CO_2 interactions that wastage effects are negligible such that an initial crack is not enlarged. Recent data from the ANL SNAKE facility has shown that at 500 °C CO_2 leaks self-plug and terminate the CO_2 release due to the formation of sodium-CO_2 reaction products. A near-term future SNAKE test will investigate whether self-plugging occurs at a lower temperature (e.g., 420 °C) representative of bulk conditions inside part of the sodium-to-CO_2 heat exchanger. SNAKE tests at lower temperatures in which large cumulative masses of CO_2 were injected into 10 cm diameter columns of sodium revealed the formation of porous agglomerated reaction products. The next SNAKE experiment will investigate CO_2 injection into a single 6 mm semicircular sodium channel.

The worldwide state-of-the-art ANL Plant Dynamics Code for steady state and transient analysis and optimization of sCO_2 cycles has been tested, improved, and validated using data from numerous tests in the small-scale sCO_2 RCBC and IST facilities. The STEP program to build and operate by 2020 a 10 MWe sCO_2 Brayton cycle pilot plant that will eliminate many of the drawbacks of small-scale facilities has been awarded.

6. Acknowledgements

Argonne National Laboratory's work was supported by the U. S. Department of Energy Advanced Reactor Technologies (ART) Program under Prime Contract No. DE-AC02-06CH11357 between the U.S. Department of Energy and UChicago Argonne, LLC. The work presented here was carried out under the Energy Conversion Technology area of the ART Program. The authors are grateful to Gary Rochau (SNL), the Technical Area Lead, Bob Hill (ANL/NE), the National Technical Director, as well as Brian Robinson (U.S. DOE), Headquarters Program Manager for the project.

7. References

[1] SIENICKI, J.J., MOISSEYTSEV, A., "Chapter 13 – Nuclear Power," Fundamentals and Applications of Supercritical Carbon Dioxide Based Power Cycles (BRUN, K., FRIEDMAN, P., Ed.), Elsevier, (2017), to be published.

[2] SIENICKI, J.J., MOISSEYTSEV, A., LV, Q., "Dry Air Cooling and the sCO_2 Brayton Cycle," GT2017-64042, Proceedings of ASME Turbo Expo 2017, Charlotte, North Carolina, USA, (June 26-30, 2017).

[3] MOISSEYTSEV, A., SIENICKI, J.J., "Development of a Plant Dynamics Computer Code for Analysis of a Supercritical Carbon Dioxide Brayton Cycle Energy Converter Coupled to a Natural Circulation Lead-Cooled Fast Reactor," ANL-06/27, Argonne National Laboratory, (July 2006).

[4] See http://www.harscoaxc.com/

[5] MOISSEYTSEV, A., LV, Q., SIENICKI, J.J., "Heat Exchanger Options for Dry Air Cooling for the sCO_2 Brayton Cycle," GT2017-63187, Proceedings of ASME Turbo Expo 2017, Charlotte, North Carolina, USA, (June 26-30, 2017).

[6] MOISSEYTSEV, A., SIENICKI, J.J., "Cost-Based Optimization of Supercritical Carbon Dioxide Brayton Cycle Equipment," American Nuclear Society 2011 Winter Meeting, Washington, DC, (October 30-November 3, 2011).

[7] PIDAPARTI, S.R., HRUSKA, P.J., MOISSEYTSEV, A., SIENICKI, J.J., and RANJAN, D., "Technical and Economic Feasibility of Dry Air Cooling for the Supercritical CO_2 Brayton Cycle using Existing Technology," The 5th International Symposium – Supercritical CO_2 Power Cycles, San Antonio, TX, (March 28-31, 2016).

[8] KIM, Y.-S., "A Proposed Correlation for Critical Flow Rate of Water Flow," Nucl. Eng. Technol., 47, (2015), 135-138.

[9] SIMON, N., LATGÉ, C., GICQUEL, L., "Investigation of Sodium-Carbon Dioxide Interactions with Calorimetric Studies," Proceedings of ICAPP 2007, Nice, France, (May 13-18, 2007).

[10] ISHIKAWA, H., MIYAHARA, S., YOSHIZAWA, Y., "Experimental Study of Sodium-Carbon Dioxide Reaction," Paper 5688, Proceedings of ICAPP '05, Seoul, Korea, (May 15-19, 2005).

[11] EOH, J.-H., NO, H.C., YOO, Y.-H., JEONG, J.-Y., KIM, J.-M., KIM, S.-O., "Wastage and Self-Plugging by a Potential CO_2 Ingress in a Supercritical CO_2 Power Conversion System of an SFR," Nucl. Eng. Technol., 47, (2010), 1023-1036.

[12] GERARDI, C., BREMER, N., LOMPERSKI, S., SIENICKI, J.J., GRANDY, C., "Chemical Interaction Experiments between Supercritical Carbon Dioxide and Liquid Sodium," Proceedings of ICAPP 2015, Paper 15334, Nice, France, (May 3-6, 2015).

[13] PARK, S.H., WI, M.-H., MIN, J.H., KIM, T.-J., "Investigation of Plugging of Narrow Sodium Channels by Sodium and Carbon Dioxide Interaction," Transactions of the Korean Nuclear Society Autumn Meeting, Pyeongchang, Korea, (October 30-31, 2014).

[14] PARK, S.H., WI, M.-H., MIN, J.H., "Preliminary Plugging Tests in Narrow Sodium Channels by Sodium and Carbon Dioxide Reaction," Transactions of the Korean Nuclear Society Spring Meeting, Jeju, Korea, (May 7-8, 2015).

[15] EOH, J., Private Communication, Korea Atomic Energy Research Institute, (January 3, 2017).

[16] FANNING, T.H., "The SAS4A/SASSYS-1 Safety Analysis Code System," ANL/NE-12/4, Argonne, IL: Argonne National Laboratory, (2012).

[17] MOISSEYTSEV, A., SIENICKI, J.J., "Dynamic Analysis of S-CO_2 Cycle Control with Coupled PDC-SAS4A/SASSYS-1 Codes," Proceedings of 20th International Conference on Nuclear Engineering, ICONE-20, Anaheim, California, USA, (July 30 - August 3, 2012).

[18] MOISSEYTSEV, A., SIENICKI, J.J., "Supercritical Carbon Dioxide Brayton Cycle for SFR Applications: Optimization, Transient Analysis, and Control," IAEA-CN-199/190, FR13, Paris, France, (2013).

[19] MOISSEYTSEV, A., SIENICKI, J.J., "Recent Developments in S-CO_2 Cycle Dynamic Modeling and Analysis at ANL," The 4th International Symposium – Supercritical CO_2 Power Cycles, Pittsburgh, Pennsylvania, USA, (September 9-10, 2014).

[20] MOISSEYTSEV, A., SIENICKI, J.J., "Lessons Learned and Improvements in ANL Plant Dynamics Code Simulation of Experimental S-CO_2 Loops," Proceedings of Power & Energy 2015, San Diego, California, USA, (June 28-July 2, 2015).

[21] MOISSEYTSEV, A., SIENICKI, J.J., "Simulation of S-CO_2 Integrated System Test with ANL Plant Dynamics Code," The 5th International Symposium – Supercritical CO_2 Power Cycles, San Antonio, TX, (March 28-31, 2016).